J Biol Inorg Chem (2009) 14:101–109
DOI 10.1007/s00775-008-0427-y

ORIGINAL PAPER

Combined arene ruthenium porphyrins as chemotherapeutics and photosensitizers for cancer therapy

Frédéric Schmitt · Padavattan Govindaswamy · Olivier Zava · Georg Süss-Fink · Lucienne Juillerat-Jeanneret · Bruno Therrien

Received: 12 August 2008 / Accepted: 26 August 2008 / Published online: 23 September 2008

Abstract Mononuclear 5-(4-pyridyl)-10,15,20-triphenylporphyrin and 5-(3-pyridyl)-10,15,20-triphenylporphyrin as well as tetranuclear 5,10,15,20-tetra(4-pyridyl)porphyrin (tetra-4-pp) and 5,10,15,20-tetra(3-pyridyl)porphyrin) (tetra-3-pp) arene ruthenium(II) derivatives (arene is C_6H_5Me or *p*-$Pr^iC_6H_4Me$) were prepared and evaluated as potential dual photosensitizers and chemotherapeutics in human Me300 melanoma cells. In the absence of light, all tetranuclear complexes were cytotoxic ($IC_{50} \leq 20$ μM), while the mononuclear derivatives were not ($IC_{50} \geq 100$ μM). Kinetic studies of tritiated thymidine and tritiated leucine incorporations in cells exposed to a low concentration (5 μM) of tetranuclear *p*-cymene derivatives demonstrated a rapid inhibition of DNA synthesis, while protein synthesis was inhibited only later, suggesting arene ruthenium–DNA interactions as the initial cytotoxic process. All complexes exhibited phototoxicities toward melanoma cells when exposed to laser light of 652 nm. At low concentration (5 μM), LD_{50} of the mononuclear derivatives was between 5 and 10 J/cm^2, while for the tetranuclear derivatives LD_{50} was approximately 2.5 J/cm^2 for the $[Ru_4(\eta^6\text{-arene})_4(\text{tetra-4-pp})Cl_8]$ complexes and less than 0.5 J/cm^2 for the $[Ru_4(\eta^6\text{-arene})_4(\text{tetra-3-pp})Cl_8]$ complexes. Examination of cells under a fluorescence microscope revealed the $[Ru_4(\eta^6\text{-arene})_4(\text{tetra-4-pp})Cl_8]$ complexes as cytoplasmic aggregates, whereas the $[Ru_4(\eta^6\text{-arene})_4(\text{tetra-3-pp})Cl_8]$ complexes were homogenously dispersed in the cytoplasm. Thus, these complexes present a dual synergistic effect with good properties of both the arene ruthenium chemotherapeutics and the porphyrin photosensitizer.

Keywords Photosensitizer · Ruthenium · Cancer · Arene ligand · Antitumor agent

F. Schmitt · O. Zava · L. Juillerat-Jeanneret (✉)
Institut Universitaire de Pathologie, CHUV,
Bugnon 25, 1011 Lausanne,
Switzerland
e-mail: lucienne.juillerat@chuv.ch

P. Govindaswamy · G. Süss-Fink · B. Therrien (✉)
Institut de Chimie, Université de Neuchâtel,
Case postale 158, 2009 Neuchâtel,
Switzerland
e-mail: bruno.therrien@unine.ch

Introduction

Combined therapies to treat serious diseases have become a standard method to improve efficiency and to decrease side effects [1–4], or to prevent resistance mechanisms commonly found in classic chemotherapeutic protocols [5]. Thus, in cancer treatment, a combination of different classes of chemotherapeutic agents or a combination of chemotherapeutics with radiation is now a common form of treatment.

Photodynamic therapy is one of these emergent cancer treatments. It requires the activation of a photosensitizer by light at specific wavelengths. The excited photosensitizer interacts with intracellular oxygen to produce singlet oxygen and radical species, inducing direct tumor cell death, immune response, and damage to tumor vasculature [6]. Photosensitizers usually possess a tetrapyrrolic structure such as porphyrin derivatives and have been shown to concentrate in cancer cells [7–9]. To improve their cellular uptake and phototoxicities, photosensitizers have been coupled to a wide range of molecules. Complexes of porphyrins (hematoporphyrin, tetraphenylporphyrin) coordinated to platinum derivatives (such as cisplatin or

oxaliplatin) were developed a few years ago to combine the cytotoxicity of platinum with the photodynamic activity of porphyrins with promising anticancer effects [10–14]. However, platinum derivatives are associated with high toxicity and resistance mechanisms [15]; therefore, the use of a different metal is very appealing to overcome the drawbacks associated with platinum [16, 17]. Ruthenium is an attractive alternative to platinum, since ruthenium compounds are known to display less general toxicity than their platinum counterparts [18], but are also able to interact with DNA and proteins [19]. With the goal to combine the photodynamic action of porphyrins and the cytotoxicity of ruthenium complexes, we have recently coordinated arene ruthenium moieties to 5,10,15,20-tetra(4-pyridyl)porphyrin (tetra-4-pp) [20]. The compounds obtained have good cytotoxicities and phototoxicities toward human melanoma cancer cells. To optimize their structure and to better understand their mechanisms of action in human melanoma cells, we have now synthesized a new series of arene ruthenium porphyrin compounds containing either one or four arene ruthenium units (arene is C_6H_5Me or *p*-Pr^{i}C$_6$H$_4$Me) coordinated to 4-pyridylporphyrin or 3-pyridylporphyrin photosensitizer derivatives: 5-(4-pyridyl)-10,15,20-triphenylporphyrin (mono-4-pp); 5-(3-pyridyl)-10,15,20-triphenyl porphyrin (mono-3-pp); tetra-4-pp; 5,10,15,20-tetra(3-pyridyl)porphyrin (tetra-3-pp). The effect of these complexes was assessed as dual chemotherapeutics and photothera-peutics in human Me300 melanoma cells as a model of metastatic cancer associated with a poor prognosis.

Materials and methods

Materials

All organic solvents were degassed and saturated with nitrogen prior to use. The pyridylporphyrin derivatives (mono-4-pp, mono-3-pp, tetra-4-pp, and tetra-3-pp) were purchased from Porphyrin Systems, Germany. [Ru(η^6-C_6H_5Me)Cl_2]$_2$, [Ru(η^6-*p*-Pr^{i}C$_6$H$_4$Me)Cl_2]$_2$, [Ru$_4$(η^6-C_6H_5Me)$_4$(tetra-4-pp)Cl_8] (**5**), [Ru$_4$(η^6-*p*-Pr^{i}C$_6$H$_4$Me)$_4$(tetra-4-pp)Cl_8] (**6**), [Ru(η^6-C_6H_5Me)(C_6H_5N)Cl_2] (**9**), and [Ru(η^6-*p*-Pr^{i}C$_6$H$_4$Me)(C_6H_5N)Cl_2] (**10**) were prepared according to published methods [20–22].

Syntheses

[Ru(η^6-C_6H_5Me)(mono-4-pp)Cl_2]

A mixture of [Ru(η^6-C_6H_5Me)Cl_2]$_2$ (17 mg, 0.032 mmol) and mono-4-pp (40 mg, 0.064 mmol) was refluxed in dry methanol (20 ml) for 4 h. In refluxing methanol the only slightly soluble mono-4-pp dissolved completely as the reaction progressed, while the [Ru(η^6-C_6H_5Me)(mono-4-pp)Cl_2] (**1**) product precipitated as a brownish purple solid. The solid was filtered and washed with diethyl ether and dried in vacuo. Yield 45 mg, 80%. ^{1}H NMR (CD_2Cl_2, 400 MHz): δ (ppm) = 9.46 (dd, 2H, $^3J_{H–H}$ = 5.12 Hz, $^4J_{H–H}$ = 1.48 Hz, $H_{pyridyl}$), 8.96 (d, 2H, $H_{pyridyl}$), 8.89 (s, 8H, $H_{pyrrole}$), 8.27–8.23 (m, 6H, H_{phenyl}), 7.82 (m, 9H, H_{phenyl}), 5.87 (m, 3H, H_{arene}), 5.48 (d, 2H, $^3J_{H–H}$ = 5.88 Hz, H_{arene}), 2.33 (s, 3H, CH_3), −2.84 (s, 2H, NH). IR (cm^{-1}): 1,717 (w), 1,609 (s), 1,473 (m), 1,441 (m), 966 (s), 805 (s), 758 (m), 730 (s), 702 (s). Electrospray ionization mass spectrometry (ESI–MS) ($CH_3CN/CHCl_3$): m/z = 844.2 [**1**–Cl]$^+$. Elemental analysis (%) calc. for $C_{50}H_{37}N_5Cl_2Ru$: C 68.19, H 4.24, N 7.96; found: C 68.15, H 4.00, N 7.91.

*[Ru(η^6-*p*-Pr^{i}C$_6$H$_4$Me)(mono-4-pp)Cl_2]*

[Ru(η^6-*p*-Pr^{i}C$_6$H$_4$Me)(mono-4-pp)Cl_2] (**2**) was prepared as described for **1** using [Ru(η^6-*p*-Pr^{i}C$_6$H$_4$Me)Cl_2]$_2$ (20 mg, 0.032 mmol) and mono-4-pp (40 mg, 0.064 mmol). Yield 40 mg, 67%. ^{1}H NMR (CD_2Cl_2, 400 MHz): δ (ppm) = 9.45 (dd, 2H, $^3J_{H–H}$ = 5.12 Hz, $^4J_{H–H}$ = 1.44 Hz, $H_{pyridyl}$), 8.97 (d, 2H, $H_{pyridyl}$), 8.88 (s, 8H, $H_{pyrrole}$), 8.25 (m, 6H, H_{phenyl}), 7.82 (m, 9H, H_{phenyl}), 5.66 (d, 2H, $^3J_{H–H}$ = 6.08 Hz, H_{arene}), 5.44 (d, 2H, H_{arene}), 3.15 (sept, 1H, $^3J_{H–H}$ = 6.84 Hz, CH), 2.28 (s, 3H, CH_3), 1.46 (d, 6H, CH_3), −2.83 (s, 2H, NH). IR (cm^{-1}): 1,717 (w), 1,650 (s), 1,508 (m), 1,458 (m), 970 (s), 800 (s), 760 (m), 730 (m). ESI–MS ($CH_3CN/CHCl_3$): m/z = 886.2 [**2**–Cl]$^+$. Elemental analysis (%) calc. for $C_{53}H_{43}N_5Cl_2Ru$: C 69.05, H 4.70, N 7.63; found: C 69.08, H 4.85, N 7.41.

[Ru(η^6-C_6H_5Me)(mono-3-pp)Cl_2]

[Ru(η^6-C_6H_5Me)(mono-3-pp)Cl_2] (**3**) was prepared as described for **1** using [Ru(η^6-C_6H_5Me)Cl_2]$_2$ (17 mg, 0.032 mmol) and mono-3-pp (40 mg, 0.065 mmol). Yield 30 mg, 53%. ^{1}H NMR (CD_2Cl_2, 400 MHz): δ (ppm) = 9.95 (d, 1H, $^4J_{H–H}$ = 2.20 Hz, $H_{pyridyl}$), 9.49 (dd, 1H, $^3J_{H–H}$ = 5.84 Hz, $H_{pyridyl}$), 8.99 (d, 1H, $^3J_{H–H}$ = 4.64 Hz, $H_{pyridyl}$), 8.91 (s, 8H, $H_{pyrrole}$), 8.66 (dd, 1H, $H_{pyridyl}$), 8.25 (m, 6H, H_{phenyl}), 7.82 (m, 9H, H_{phenyl}), 5.72 (m, 3H, H_{arene}), 5.57 (m, 2H, H_{arene}), 2.17 (s, 3H, CH_3), −2.83 (s, 2H, NH). IR (cm^{-1}): 1718 (w), 1595 (m), 1474 (m), 1440 (m), 1350 (m), 966 (s), 799 (s), 730 (m), 702 (s). ESI–MS ($CH_3CN/CHCl_3$): m/z = 844.2 [**3**–Cl]$^+$. Elemental analysis (%) calc. for $C_{50}H_{37}N_5Cl_2Ru$: C 68.19, H 4.24, N 7.96; found: C 68.39, H 4.33, N 7.96.

[Ru(η^6-p-Pr^{i}C$_6$H$_4$Me)(mono-3-pp)Cl$_2$]

[Ru(η^6-*p*-Pr^{i}C$_6$H$_4$Me)(mono-3-pp)Cl$_2$] (**4**) was prepared as described for **1** using [Ru(η^6-*p*-Pr^{i}C$_6$H$_4$Me)Cl$_2$]$_2$ (20 mg, 0.032 mmol) and mono-3-pp (40 mg, 0.064 mmol). Yield 35 mg, 58%. ^{1}H NMR (CD_2Cl_2, 400 MHz): δ (ppm) = 9.92 (d, 1H, $^4J_{H-H}$ = 1.96 Hz, $H_{pyridyl}$), 9.47 (dd, 1H, $^3J_{H-H}$ = 5.68 Hz, $H_{pyridyl}$), 8.99 (d, 1H, $^3J_{H-H}$ = 4.84 Hz, $H_{pyridyl}$), 8.91 (s, 8H, $H_{pyrrole}$), 8.64 (dd, 1H, $H_{pyridyl}$), 8.25 (m, 6H, H_{phenyl}), 7.82 (m, 9H, H_{phenyl}), 5.55 (d, 2H, $^3J_{H-H}$ = 6.16 Hz, H_{arene}), 5.29 (d, 2H, H_{arene}), 3.01 (sept, 1H, $^3J_{H-H}$ = 7.04 Hz, CH), 2.12 (s, 3H, CH_3), 1.32 (d, 6H, CH_3), −2.83 (s, 2H, NH). IR (cm^{-1}): 1,717 (w), 1,624 (w), 1,508 (m), 1,474 (m), 967 (s), 800 (s), 731 (m), 702 (s). ESI–MS ($CH_3CN/CHCl_3$): *m*/*z* = 886.2 [**1**–Cl]$^+$. Elemental analysis (%) calc. for $C_{53}H_{43}N_5Cl_2Ru$: C 69.05, H 4.70, N 7.63; found: C 69.10, H 4.78, N 7.30.

[Ru$_4$(η^6-C$_6$H$_5$Me)$_4$(tetra-3-pp)Cl$_8$]

[Ru$_4$(η^6-C_6H_5Me)$_4$(tetra-3-pp)Cl_8] (**7**) was prepared as described for **1** using [Ru(η^6-C_6H_5Me)Cl_2]$_2$ (70 mg, 0.13 mmol) in excess and tetra-3-pp (40 mg, 0.064 mmol). Yield 85 mg, 77%. ^{1}H NMR (dimethyl sulfoxide-d_6, DMSO-d_6,, 400 MHz): δ (ppm) = 9.41 (d, 4H, $^3J_{H-H}$ = 5.08 Hz, $H_{pyridyl}$), 9.09 (d, 4H, $^4J_{H-H}$ = 1.48 Hz, $H_{pyridyl}$), 8.90 (s, 8H, $H_{pyrrole}$), 8.70 (d, 4H, $^3J_{H-H}$ = 6.54 Hz, $H_{pyridyl}$), 7.94 (dd, 4H, $H_{pyridyl}$), 5.98 (m, 8H, H_{arene}), 5.71 (m, 12H, H_{arene}), 2.14 (s, 12H, CH_3), −2.96 (s, 2H, NH). IR (cm^{-1}): 1,717 (w), 1,637 (s), 1,508 (s), 1,458 (m), 1,406 (s), 968 (m), 796 (m), 730 (w), 702 (w). ESI-MS ($CH_3CN/CHCl_3$): *m*/*z* = 492.9 [**7**–C_6H_5Me–3 Cl]$^{3+}$. Elemental analysis (%) calc. for $C_{68}H_{58}N_8Cl_8Ru_4$: C 48.76, H 3.49, N 6.69; found: C 48.39, H 3.40, N 6.77.

[Ru$_4$(η^6-p-Pr^{i}C$_6$H$_4$Me)$_4$(tetra-3-pp)Cl$_8$]

[Ru$_4$(η^6-*p*-Pr^{i}C$_6$H$_4$Me)$_4$(tetra-3-pp)Cl$_8$] (**8**) was prepared as described for **1** using [Ru(η^6-*p*-Pr^{i}C$_6$H$_4$Me)Cl$_2$]$_2$ (60 mg, 0.098 mmol) in excess and tetra-3-pp (30 mg, 0.049 mmol). Yield 70 mg, 78%. ^{1}H NMR (CD_2Cl_2, 400 MHz): δ (ppm) = 9.93 (d, 4H, $^3J_{H-H}$ = 7.76 Hz, $H_{pyridyl}$), 9.48 (d, 4H, $^4J_{H-H}$ = 1.08 Hz, $H_{pyridyl}$), 9.06 (s, 8H, $H_{pyrrole}$), 8.68 (d, 4H, $^3J_{H-H}$ = 7.00 Hz, $H_{pyridyl}$), 7.85 (dd, 4H, $H_{pyridyl}$), 5.56 (d, 8H, $^3J_{H-H}$ = 5.92 Hz, H_{arene}), 5.32 (d, 8H, H_{arene}), 3.02 (sept, 4H, $^3J_{H-H}$ = 6.68 Hz, CH), 2.15 (s, 12H, CH_3), 1.32 (s, 24H, CH_3), −2.90 (s, 2H, NH). IR (cm^{-1}): 1717 (w), 1,682 (m), 1,637 (s), 1,508 (s), 1,458 (s), 1,406 (s), 970 (m), 795 (m), 730 (w). ESI–MS ($CH_3CN/CHCl_3$): *m*/*z* = 578.9 [**8**–3 Cl]$^{3+}$. Elemental analysis (%) calc. for $C_{80}H_{82}N_8Cl_8Ru_4$: C 52.12, H 4.48, N 6.08; found: C 52.53, H 4.52, N 6.03.

Spectroscopic methods

NMR spectra were recorded using a Varian 400 MHz spectrometer. IR spectra were recorded in KBr pellets with a PerkinElmer 1720X Fourier transform IR spectrometer (4,000–400 cm^{-1}). Microanalyses were performed by the Laboratory of Pharmaceutical Chemistry, University of Geneva (Switzerland). Electrospray mass spectra were obtained in positive-ion mode with a Finnigan LCQ mass spectrometer (University of Fribourg, Switzerland). UV–vis absorption spectra were recorded using a Uvikon 930 spectrophotometer. Quantum yields were assessed after excitation at 414 nm. Fluorescence quantum yields at 648 nm were determined using a PerkinElmer LS50 spectrofluorometer. The singlet oxygen quantum yield was determined using the singlet oxygen specific fluorescence at 1,270 nm monitored by a liquid-nitrogen-cooled germanium detector (model EO-817L, North Coast Scientific) from the DCPR facility, ENSIC, Nancy, France.

Cell culture

Human Me300 melanoma cells were kindly provided by D. Rimoldi (Ludwig Institute of Cancer Research, Lausanne branch, Switzerland). All cell culture reagents were obtained from Gibco-BRL (Basel, Switzerland). The cells were grown in RPMI 1640 medium containing 10% of heat-inactivated fetal calf serum and penicillin/streptomycin. The organometallic complexes were dissolved in DMSO as the stock solution and then diluted in complete medium to the required concentration immediately prior to use. The final DMSO concentration never exceeded 1% v/v and this concentration did not show any effects on cell viability (results not shown).

Determination of dark cytotoxicity

Cells were grown in 48-well cell culture plates (Corning, NY, USA) until they were 20% confluent. The culture medium was replaced with complete medium containing the ruthenium complexes for concentrations from 0 to 100 μM and the cells were exposed to the complexes for 72 h. Thereafter, cell survival was measured using the alamarBlue test as previously described [23, 24]. In accordance with the manufacturer's instructions, alamarBlue solution (AbD Serotec, Oxon, UK) was added at 10% v/v and incubation was continued for 2 h. Fluorescence intensities of the cell culture supernatants were assessed using a fluorescence microplate reader (Cytofluor, PerSeptive BioSystems, Switzerland) at excitation and emission wavelengths of 530 and 580 nm, respectively. The values for treated cells were compared with the values

for control cells incubated without complexes. Experiments were conducted in triplicate wells and repeated at least twice.

Kinetic evaluation of DNA and protein syntheses

Thymidine incorporation and leucine incorporation were used to assess DNA and protein synthesis, respectively, as previously described [25]. Cells were grown in 48-well cell culture plates (Corning, NY, USA) until they were 20% confluent. The culture medium was replaced with complete medium containing the ruthenium complexes at 5 μM concentration and cells were exposed to the complexes for different times (0–72 h). Cell survival and tritiated thymidine (^{3}H-T) or tritiated leucine (^{3}H-Leu) incorporations were assessed by incubating the cells for a further 2 h period with ^{3}H-T (Amersham-Pharmacia, Dübendorf, Switzerland; 400 nCi/mL) or ^{3}H-Leu (American Radiolabeled Chemicals, St Louis, MO, USA; 400 nCi/mL) together with the alamarBlue solution as described earlier, as a multiplex experiment. After the assessment of cell survival, the cell layer was washed, precipitated with 10% trichloracetic acid, and the precipitate was dissolved in 1% sodium dodecyl sulfate/0.1 N NaOH. Radioactivity was counted using a β-counter (WinSpectral, Wallac Regensdorf, Switzerland) after the addition of a scintillation cocktail (Optiphase HI-Safe, PerkinElmer). The values for treated cells were compared with the values for control cells incubated without complexes. Experiments were conducted in triplicate wells and repeated at least twice.

Determination of phototoxicity

Cells were grown in 96-well cell culture plates (Costar) until they were 20% confluent. The culture medium was replaced with complete medium containing ruthenium complexes **1**–**8** at 5 μM concentration and the cells were exposed to the complexes for 24 h. Thereafter, cells were irradiated at 652 nm using a diode laser (Ceralas 652, Biolitec, Germany) coupled to a frontal diffuser (Medlight, Ecublens, Switzerland), at an irradiance of 20 mW/cm^2 and light doses ranging between 0.5 and 20 J/cm^2. Experiments were conducted in triplicate. Analysis of cell viability using the alamarBlue assay as described before was performed after a further incubation period of 48 h and the values obtained were compared with the values for control cells.

Fluorescence microscopy

Cells were grown on histology slides in complete medium until they were 25% confluent and were then exposed to compound **5** or **7** (5 μM) for 24 h in the dark. Nuclei were stained with 4′,6′-diamidino-2-phenylindolylhydrochloride (DAPI; 1 mg/L, Roche Diagnostics, Mannheim, Germany) in phosphate-buffered saline. Alternatively, Lysotracker (500 nM, Invitrogen, Paisley, UK) or rhodamine 123 (500 μM, Fluka, Buchs, Switzerland) were incubated with DAPI for the organelle localization studies. Slides were mounted in phosphate-buffered saline and analyzed under a fluorescence microscope (Axioplan2, Carl Zeiss, Feldbach, Switzerland) with filters set at 365 ± 5 nm excitation light (BP 365/12, FT 395, LP 397) for DAPI, 535 ± 25 nm excitation light (BP 510–560, FT 580, LP 590) for porphyrins, and 470 ± 20 nm excitation light (BP 450–490, FT 510, BP 515–565) for Lysotracker and rhodamine 123.

Results

Syntheses

The dinuclear arene ruthenium complexes [Ru(η^6-arene)Cl$_2$]$_2$ (arene is C_6H_5Me or p-Pr^{i}C$_6$H$_4$Me) react in refluxing methanol with monopyridylporphyrin (mono-3-pp or mono-4-pp) to give the corresponding mononuclear complexes **1**–**4** (Scheme 1).

Similarly, 2 equiv of dinuclear arene ruthenium complexes reacts in refluxing methanol with tetra-3-pp to give the corresponding tetranuclear arene ruthenium complexes **7** and **8** (Scheme 2).

The previously reported [20–22] complexes **5** and **6** and the simple monopyridyl arene ruthenium derivatives **9** and **10**, depicted in Fig. 1, were also included in this study.

The ^{1}H NMR spectra of **1**–**8** were recorded in DMSO-d_6 owing to the low solubility of the complexes in water. All complexes show, in addition to the signals of the corresponding η^6-arene signals for the organometallic parts and two multiplets centered at $\delta = 8.2$ and $\delta = 7.8$ ppm for the phenyl groups, the typical three-signal pattern for the pyrrolyl and pyridyl protons of the porphyrin unit between $\delta = 9.5$ and $\delta = 8.0$ ppm, the pyridyl signals being observed as two doublets, while the pyrrolyl protons give a singlet. The two NH protons appear upfield as a singlet at $\delta \sim -2.9$ ppm.

The IR spectra of **1**–**8** in KBr pellets show weak N–H stretching vibrations above 3,300 cm^{-1} in the high wavenumber region. In the mid-frequency region, porphyrin skeletal stretching and C=N pyrrole stretching bands are observed at 1,720, 1,650, 1,600, 1,510, 1,460, and 1,400 cm^{-1}, while in the low wavenumber region, the in-plane bending, out-of-plane bending, ring rotation, and ring torsion modes of the pyridylporphyrin skeletal are found at 970, 800, 730, and 700 cm^{-1}.

Wavelengths and extinction coefficients of absorption bands of **1**–**8** in dichloromethane are presented in Table 1,

Scheme 1 Synthesis of monopyridylporphyrin compounds **1–4**

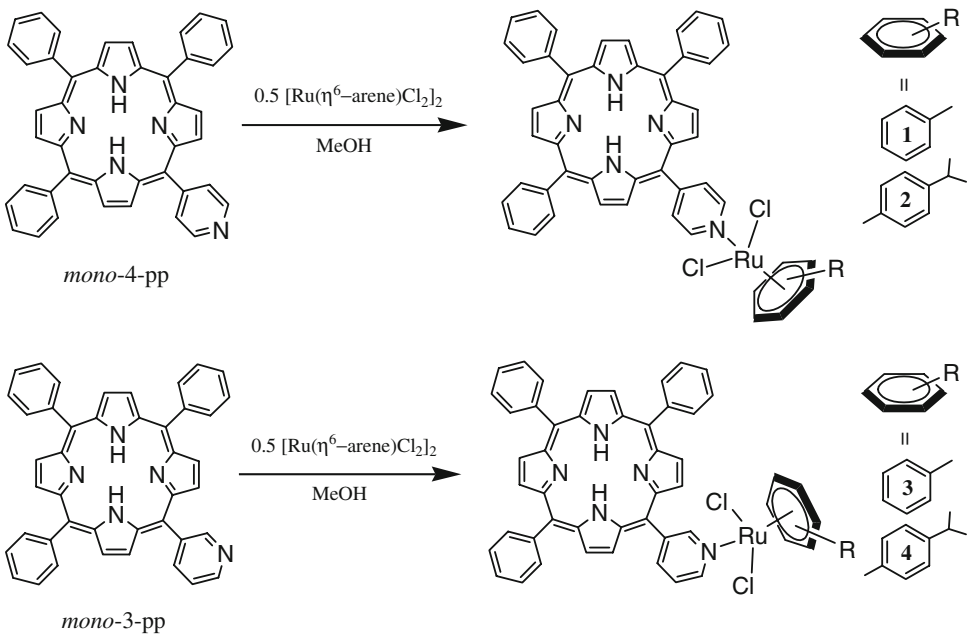

Scheme 2 Synthesis of tetrapyridylporphyrin compounds **7** and **8**

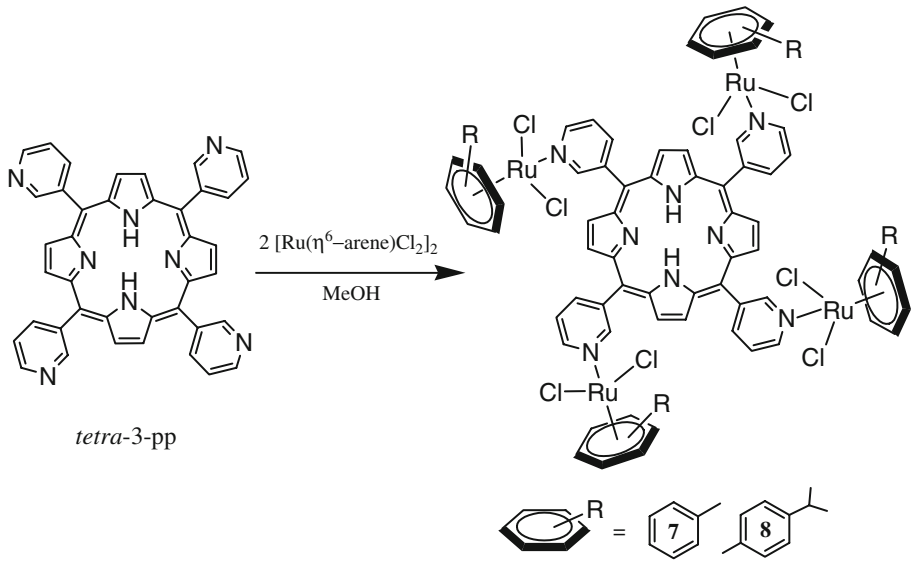

Fig. 1 Constitution of compounds **5**, **6**, **9**, and **10** [20–22]

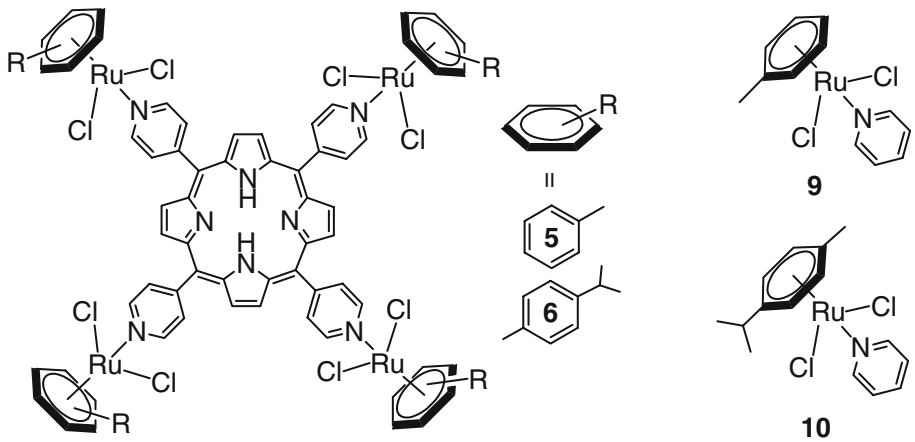

Table 1 UV–vis maximum absorption and molar extinction coefficients [λ ($\varepsilon \times 10^{-3}$ M^{-1} cm^{-1})] determined in CH_2Cl_2, fluorescence quantum yields at 648 nm (ϕ_f^{648}) in MeOH and singlet oxygen quantum yields $\phi_{O_2}^1$ in EtOH

Complex	Soret band	Q band IV	Q band III	Q band II	Q band I	ϕ_f^{648} (%)	$\phi_{O_2}^1$ (%)
1	418 (167.2)	515 (12.7)	551 (7.1)	590 (5.4)	646 (4.5)	10.9	49
2	419 (153.6)	515 (10.0)	551 (5.8)	589 (4.6)	645 (3.7)	9.8	81
3	419 (156.7)	515 (10.0)	550 (5.1)	589 (4.2)	645 (3.4)	9.5	41
4	418 (162.4)	515 (11.3)	549 (5.3)	589 (4.1)	646 (4.0)	11.3	64
5	423 (156.5)	516 (13.6)	550 (7.7)	590 (6.7)	645 (4.4)	7.4	66
6	422 (188.2)	515 (19.8)	550 (9.1)	590 (6.9)	645 (4.8)	7.9	76
7	423 (151.1)	516 (12.2)	550 (6.7)	590 (5.5)	646 (4.3)	8.1	70
8	423 (158.4)	516 (11.1)	550 (5.1)	589 (4.6)	646 (2.9)	7.6	79

See "Materials and methods" for the description of the complexes

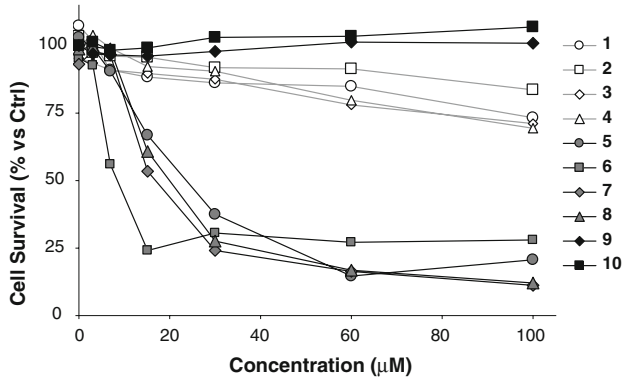

Fig. 2 Concentration dependence of the growth inhibition of organometallic porphyrin compounds in human Me300 melanoma cells. Cells were exposed to compounds **1**–**10** in the dark for 72 h, then the amount of metabolically active cells was determined by the alamarBlue assay (standard deviations are not shown for the purpose of clarity but did not exceed ±5%)

together with fluorescence and singlet oxygen quantum yields measured after 414-nm excitation. Like the parent porphyrins, complexes **1**–**8** exhibit the four Q bands between 510 and 650 nm and the intense Soret-type band around 420 nm. Interestingly, despite structural differences, all tetrapyridyl derivatives (**5**–**8**) show similar oxygen quantum yields in methanol.

Biological assays

The growth inhibition exerted by these new organometallic porphyrin complexes was investigated in vitro using human Me300 melanoma cells. Cells were exposed for 72 h to increasing concentrations of compounds **1**–**10** and their survival was determined using the alamarBlue assay. In the absence of laser exposure (dark toxicity), compounds **1**–**4**, bearing one ruthenium moiety, inhibited poorly the growth of melanoma cells, while compounds **5**–**8**, bearing four ruthenium moieties, were potent growth inhibitors ($IC_{50} \sim 20$ μM for **5**, **7**, and **8** and $IC_{50} \sim 10$ μM for **6**). The corresponding monopyridyl arene ruthenium derivatives **9** and **10** did not display any cytotoxic effect (Fig. 2).

The potential of the complexes to decrease cell growth by inhibiting the synthesis of DNA and/or proteins was also determined. Me300 melanoma cells were incubated with complexes **6** and **8** at 5 μM concentrations (below IC_{50}) and the incorporations of ^{3}H-T or ^{3}H-Leu were evaluated at different incubation times. Exposure of the cells to these molecules demonstrated that they inhibited thymidine incorporation (DNA synthesis) very rapidly (less than 3 h) and that thymidine incorporation was completely inhibited after 5 h of cell exposure (Fig. 3a). Leucine incorporation was only slightly blocked by the complexes (Fig. 3b).

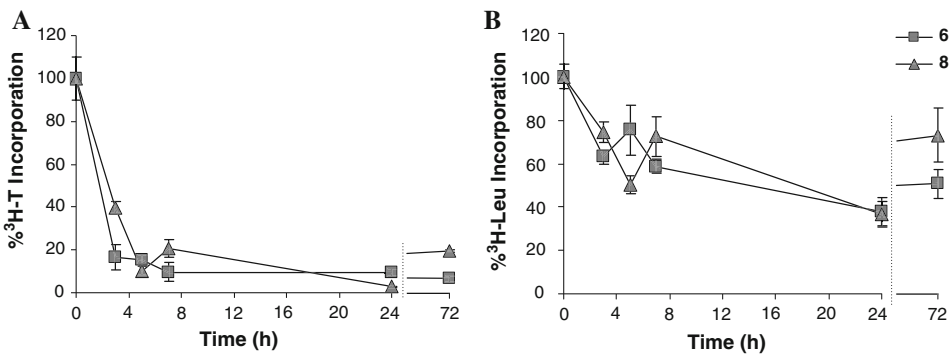

Fig. 3 DNA and protein syntheses in human Me300 melanoma cells exposed to complexe **6** or **8** at 5 μM concentration. Cells were exposed to compound **6** or **8** in the dark and the evaluation of the incorporation of either **a** tritiated thymidine (^{3}H-T) or **b** tritiated leucine (^{3}H-Leu) was performed after different times of incubation

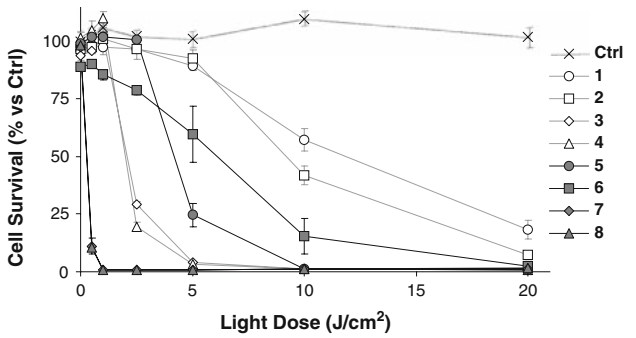

Fig. 4 Photodynamic activity of compounds **1**–**8** in human Me300 melanoma cells. Cells were exposed to compounds **1**–**8** (5 μM) in the dark for 24 h, before being exposed to increasing doses of light at 652-nm wavelength. Then the amount of metabolically active cells was determined 48 h later by the alamarBlue assay. Cells not exposed to the compounds, but irradiated, were used as controls

Similarly, the phototoxic efficacy of the porphyrin complexes was assessed at 5 μM concentrations. Cells were incubated for 24 h with compounds **1**–**8** before irradiation at 652 nm (20 mW/cm^2), then alamarBlue assay was performed after a further incubation of 48 h. The phototoxic efficacy of the compounds was related to the porphyrin structures and not to the nature of the arene moieties. For the tetranuclear arene ruthenium 3-pyridylporphyrins **7** and **8,** LD_{50} was less than 0.5 J/cm^2, for the mononuclear arene ruthenium 3-pyridylporphyrins **3** and **4,** $LD_{50} = 2.5$ J/cm^2, for tetranuclear arene ruthenium 4-pyridylporphyrins **5** and **6**, $LD_{50} = 5.0$ J/cm^2, and for mononuclear arene ruthenium 4-pyridylporphyrins **1** and **2**, $LD_{50} = 10$ J/cm^2 (Fig. 4).

The uptake by Me300 melanoma cells of the tetranuclear compounds **5** and **7** at 5 μM concentration was determined after 24 h of cell exposure, using fluorescence microscopy (Fig. 5). The fluorescence associated with porphyrins **5** and **7** appears red, whereas cell nuclei appear blue with DAPI counterstaining. The two compounds displayed a very different pattern of accumulation in the cytoplasm of melanoma cells. Compound **5** was visible as red fluorescent spots, as previously described [20], while the fluorescence of compound **7** was homogenously distributed in the cytoplasm. For both compounds, nuclear fragmentation was not observed, suggesting the absence of cell apoptosis during this time course. Intracellular localization studies with fluorescent reporter probes for lysosomes and mitochondria (Lysotracker and rhodamine 123, respectively) revealed that **5** and **7** did not preferentially localize in these organelles (results not shown).

Discussion

Dual chemotherapeutic agents combining two independent therapeutic modalities with anticancer potential are advantageous for therapeutic efficacy and to overcome resistance mechanisms. In the present study, our aim was to develop molecules able to combine the photosensitizing properties of porphyrins with the chemotherapeutic effects of ruthenium, as potential drug candidates for cancer therapy. Thus, new porphyrin arene ruthenium complexes, bearing one or four arene ruthenium moieties coupled to 4-pyridylporphyrin or 3-pyridylporphyrin, were synthesized according to a previously described procedure [20].

All compounds presented similar spectroscopic properties. The electron-withdrawing character of the pyridyl groups in the 3-pyridylporphyrin derivatives was stronger than in the 4-pyridylporphyrin systems; thus, the ratios of intensities of bands III and II ($\varepsilon_{3\text{-pp}}/\varepsilon_{4\text{-pp}}$) followed the same order [26]. Arene ruthenium groups increased the hydrophilicity of the highly hydrophobic pyridylporphyrin ligands and thus allowed their solubilization in polar organic solvents, whereas the free pyridylporphyrins were nearly insoluble in polar solvents, including DMSO.

The evaluation of such compounds as chemotherapeutic agents and phototherapeutic agents in photodynamic therapy was done using human Me300 melanoma cells. All

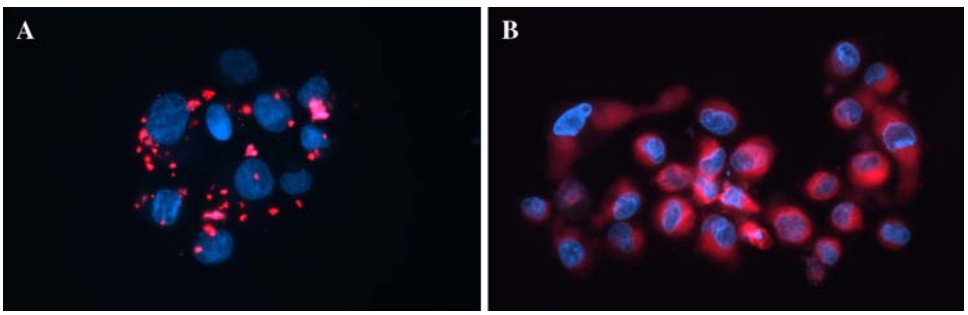

Fig. 5 Accumulation of tetranuclear arene ruthenium porphyrin compounds in human Me300 melanoma cells by fluorescence microscopy. Cells were grown on histology glass slides and were exposed to compound **5** (**a**) or **7** (**b**) at 5 μM concentration for 24 h in the dark. Compounds **5** and **7** appear as red fluorescence spots and cell nuclei as blue fluorescence after 4′,6′-diamidino-2-phenylindolylhydrochloride counterstaining

compounds possessed distinct cell growth inhibitory profiles, which was always linked to the functionalization of the tetrapyrrole ring. Compounds bearing only one arene ruthenium moiety were only slightly cytotoxic in the absence of laser irradiation, displaying LC_{50} values greater than 100 μM, whereas tetranucleated compounds were good inhibitors of cell growth, presenting LD_{50} values of 20 μM or less. The porphyrin ring also seemed to play a role in this process, maybe responsible for the intracellular localization of the compounds or increasing their hydrophobicity. With the aim to evaluate the intracellular target of the tetranucleated complexes, kinetic evaluations of DNA and protein synthesis were assessed at noncytotoxic concentrations (5 μM) of these compounds. Exposure of melanoma cells to these molecules demonstrated that they rapidly inhibit DNA synthesis, while the inhibition of protein synthesis was a later event and was only partial. These results suggested a cytotoxic effect of these molecules initially by inhibiting DNA synthesis, which will induce a decrease of protein synthesis resulting in diminished cell survival. This pattern corresponds to the effects described for some platinum or other ruthenium derivatives known to bind to DNA [27–32].

Photodynamic studies revealed that the nature of the pyridylporphyrin isomer (3-pyridyl or 4-pyridyl) was more important than the degree of substitution of the tetrapyrrole ring. With similar spectroscopic properties, 3-pyridyl photosensitizers were more photosensitizing than 4-pyridyl photosensitizers at an equivalent degree of substitution. The mononuclear 3-pyridyl complexes (**3** and **4**) were even better photosensitizers than the tetranuclear 4-pyridyl complexes (**5** and **6**). Hence, the best combination (compounds **7** and **8**) was composed of four arene ruthenium groups coordinated to the tetradentate tetra-3-pp ligand. Such compounds only needed very low light doses (less than 0.5 J/cm^2) and low concentration (5 μM) to induce cell death.

Fluorescence microscopy studies demonstrated that the tetranuclear complexes presented a very different pattern of accumulation in the cytoplasm depending on the particular isomer of tetrapyridylporphyrin. Compound **5**, bearing a tetra-4-pp group, was found as red fluorescent spots in the cell cytoplasm as previously observed [20], while the fluorescence associated with the tetra-3-pp derivative (**7**) was found to be homogenously distributed in the cytoplasm. We associated this pattern of cellular localization with the important differences in photosensitizing efficacy. We observed that free tetra-3-pp was more soluble in DMSO than free tetra-4-pp. This information suggests that the increased hydrophobicity of the latter compound resulted in an increased propensity to aggregate in an aqueous medium, as observed for compound **5** under the microscope, resulting in a lower photodynamic efficacy, since aggregates decrease the formation of singlet oxygen [33].

In conclusion, we prepared a series of new organometallic-modified porphyrin compounds and showed that they present a synergistic effect with good properties of both the arene ruthenium chemotherapeutic effect and the porphyrinic photosensitizing efficiency at low concentration (5 μM) and low dose of red light (less than 0.5 J/cm^2 at 652 nm). Moreover, we showed that the ruthenium porphyrin compounds accumulated differently in the cytoplasm depending on the particular porphyrin they are composed of, inducing different phototoxicity, however with identical spectroscopic properties.

Acknowledgments We thank C. Frochot and S. Hupont (DCPR, ENSIC, Nancy, France) for their assistance in determining the singlet oxygen quantum yields and C. Frochot for helpful discussions. This work was financially supported by the Swiss Commission for Technology and Innovation CTI grant no. 7985.2 and COST program D39 "Metallo-drug design and action". O.Z. was financially supported by the BNF program of Switzerland. We thank the Fondation Suisse pour la Lutte Contre le Cancer (grant no. 227) for financing the purchase of the photodynamic therapy laser and Johnson Matthey Research Centre for a generous loan of ruthenium chloride hydrate.

References

1. Pepper DJ, Meintjes GA, McIlleron H, Wilkinson RJ (2007) Drug Discov Today 12:980–989
2. Franklin RA, Libra M, Stivala F, McCubrey JA (2005) Cancer Biol Ther 4:1190–1191
3. Stein JA, Brownell I (2008) J Drugs Dermatol 7:175–179
4. Lorigan P, Eisen T, Hauschild A (2008) Exp Dermatol 17:383–394
5. Szakacs G, Paterson JK, Ludwig JA, Booth-Genthe C, Gottesman MM (2006) Nate Rev Drug Discov 5:219–234
6. Dolmans DEJGJ, Fukumura D, Jain RK (2003) Nat Rev Cancer 3:380–387
7. Juillerat-Jeanneret L (2006) Trends Cancer Res 2:71–84
8. Barrrett AJ, Kennedy JC, Jones RA, Nadeau P, Pottier RH (1990) J Photochem Photobiol B 6:309–323
9. Nyman ES, Hynninen PH (2004) J Photochem Photobiol B 73: 1–28
10. Lottner C, Bart KC, Bernhardt G, Brunner H (2002) J Med Chem 45:2064–2078
11. Lottner C, Bart KC, Bernhardt G, Brunner H (2002) J Med Chem 45:2079–2089
12. Kim YS, Song R, Kim DH, Jun MJ, Sohn YS (2003) Bioorg Med Chem 11:1753–1760
13. Lottner C, Knuechel R, Bernhardt G, Brunner H (2004) Cancer Lett 203:171–180
14. Hamblin MR, Newman EL (1994) J Photochem Photobiol B 26:45–56
15. Wong E, Giandomenico CM (1999) Chem Rev 99:2451–2466
16. Hannon MJ (2007) Pure Appl Chem 79:2243–2261
17. Jaouen G (ed) (2006) Bioorganometallics. Wiley, Weinheim
18. Ang WH, Dyson PJ (2006) Eur J Inorg Chem 4003–4018
19. Melchart M, Sadler PJ (2006) In: Jaouen G (ed) Bioorganometallics. Wiley, Weinheim, pp 50–61

20. Schmitt F, Govindaswamy P, Süss-Fink G, Ang WH, Dyson PJ, Juillerat-Jeanneret L, Therrien B (2008) J Med Chem 51: 1811–1816
21. Bennett MA, Smith AK (1974) J Chem Soc Dalton Trans 233–241
22. Vock CA, Scolaro C, Phillips AD, Scopelliti R, Sava G, Dyson PJ (2006) J Med Chem 46:5552–5561
23. Nociari MM, Shalev A, Benias P, Russo C (1998) J Immunol Methods 213:157–167
24. Vallinayagam R, Schmitt F, Barge J, Wagnières G, Wenger V, Neier R, Juillerat-Jeanneret L (2008) Bioconjug Chem 19: 821–839
25. Fiaux H, Popowycz F, Favre S, Schütz C, Vogel P, Gerber-Lemaire S, Juillerat-Jeanneret L (2005) J Med Chem 48: 4237–4246
26. Sugata S, Yamanouchi S, Matsushima Y (1977) Chem Pharm Bull 25:884–889
27. Perrin LC, Prenzler PD, Cullinane C, Phillips DR, Denny WA, McFayed WD (2000) J Inorg Biochem 81:111–117
28. Aldrich-Wright J, Brodie C, Glazer EC, Luedtke NW, Elson-Schwab L, Tor Y (2004) Chem Commun 1018–1019
29. Liu YJ, Chao H, Tan LF, Yuan YX, Wei W, Ji LN (2005) J Inorg Biochem 99:530–537
30. Swavey S, Brewer KJ (2002) Inorg Chem 41:6196–6198
31. Davia K, King D, Hong Y, Swavey S (2008) Inorg Chem Commun 11:584–586
32. Toma HE (2003) J Braz Chem Soc 14:845–869
33. Boyle RW, Dolphin D (1996) Photochem Photobiol 64:469–485